



On modelling the kinematics and evolutionary properties of pressure pulse driven impulsive solar jets

Balveer Singh, Kushagra Sharma, and Abhishek K. Srivastava

Department of Physics, Indian Institute of Technology (BHU), Varanasi-221005, India.

Correspondence: Balveer Singh (balveersingh.rs.phy17@itbhu.ac.in)

Abstract. In this paper, we describe the kinematical and evolutionary properties of the impulsive solar jets using numerical simulation by Godunov-type PLUTO code. These type of chromospheric jets are originated by the pressure pulse, which mimics the after effects of the localized heating in the lower solar atmosphere. These jets may responsible for the transporting of mass and energy in the localized upper atmosphere (i.e., corona). The automated detection of height-time profiles for the jets originated by imposing the different pressure pulses exhibit the asymmetric near parabolic profiles. This infers that the upward motion of the jet occurs under the influence of pressure perturbation. However, its downward motion is not only governed by the gravitational free fall but also due to the complex plasma motions near its base due to the counter propagating pulses. Maximum height and life-time of the jets w.r.t. strength of the pressure pulse show a linear increasing trend. This suggests that if the extent of the heating and thus pressure perturbations will be higher then more longer chromospheric jets can be triggered from the same location in the chromosphere. Although, we present the kinematics and evolutionary properties of the a isolated jets, but usually such jet triggering sites with pressure perturbations exhibits the formation of the multiple jets along with the significant brightening at their base. In conclusions, our model mimics the properties and evolution of the impulsive jets (e.g., macrospicules, network jets, isolated repeated cool jets, confined & small surges etc).

15 1 Introduction

Observations reveal that various types of plasma jets are ubiquitous in the solar atmosphere at diverse spatio-temporal scales (e.g., Sterling 2000; Katsukawa et al. 2007; Shibata et al. 2007; Nisticò et al. 2009; Wedemeyer-Böhm et al. 2012; Tian et al. 2014; Raouafi et al. 2016, Kayshap et al. 2018, and references cited therein). These jets are significant in transporting energy and mass in the localized upper atmosphere (i.e., corona) of the Sun. As far as the complex magnetic structuring of the solar chromosphere is concerned, it triggers various types of cool plasma jets (e.g., spicules, macrospicules, surges, magnetic swirls, network jets, evolution of plasma twists etc), which attribute to the association of exotic wave and plasma processes (e.g., De Pontieu et al. 2004, 2007, 2014; McIntosh et al. 2011; Wedemeyer-Böhm et al. 2012, Tian et al. 2014, Kayshap et al. 2018, Srivastava et al. 2017, 2018, and references cited therein).



In the recent observations, it is found that quiet solar chromosphere triggers various kinds of localized solar jets (e.g., magnetic swirls, network jets, spicule-like rotating plasma structures, etc) apart from the typical spicules (e.g., Wedemeyer-Böhm et al. 2012; Tian et al. 2014; Shetye et al. 2016, and references cited therein). Moreover, solar macrospicules, confined surges, anemone jets etc are also some other flowing magnetic structures typically observed in the solar chromosphere (e.g., Roy 1973; Wilhelm 2000; Morita et al. 2010, and references cited therein). The evolution of such a variety of chromospheric jets at diverse spatio-temporal scales provides a very detailed picture of the ongoing different plasma processes triggering these jets in an abundant measure in the localized solar atmosphere (e.g., De Pontieu et al. 2004, 2007; McIntosh et al. 2011; Kayshap et al. 2013; Murawski et al. 2011, 2018, Srivastava et al. 2017; Martínez-Sykora et al. 2017; Iijima & Yokoyama 2017; Kayshap et al. 2018, and references cited therein).

It is well established that complex magnetic structuring of the solar chromosphere enables small-scale magnetic reconnection and thus the localized heating and generation of the solar jets (e.g., Yokoyama & Shibata 1995). However, the height of the reconnection and its magnitude decides the evolution of the inherent physical processes. If the reconnection occurs in the chromosphere, then the evolution of shocks and plasma motion may be evident (e.g., Shibata et al. 1992; Kayshap et al. 2013a, and references cited therein). However, the reconnection height lying in the inner corona may result in the jet propagation due to direct influence of the Lorentz force, and Alfvén waves can also be evolved (e.g., Nishizuka et al. 2008, Jelińek et al. 2016, and references cited therein).

Recently, observations and modeling of the chromosphere revealed that many localized jets (e.g., spicules and macrospicules, network jets, confined surges, jets in the twisted or straight magnetic spires, chromospheric jets near flare ribbons etc) exhibit the brightening and heating at their footpoints before their evolution (e.g., Isobe et al. 2007; Murawski et al. 2011; Uddin et al. 2012; Kayshap et al. 2013b, 2018; Li et al. 2019, and references cited therein). Recent observations reveal that the network jets are found to be associated with the impulsive origin in the chromosphere (Kayshap et al. 2018), and they morphologically overlap with each other and type-I/type-II spicules as well in the quiet Sun chromosphere (Tian et al. 2014). In the present paper, we present a model of the pressure-pulse driven jets and their evolutionary properties, which may mimic the variety of impulsive chromospheric jets (e.g., macro spicules, network jets, confined smaller jet-like surges) originating at the top of the photosphere. The pressure pulse acts as a driver mimicking that heating is already occurred which has activated the pressure perturbations launching the jets. In Sect. 2, we describe the MHD model of the jet, solar atmosphere, perturbations, and numerical methods. The results are described in Sect. 3. The discussion and conclusion is outlined in the last section.

2 MHD Model of the Pressure Pulse Driven Jets

In order to model the jets, We consider a gravitationally-stratified and magnetized solar atmosphere which is approximated by the ideal MHD equations in their conservative form as outlined below (Mignone et al., 2007, 2012, Wołoszkiewicz et al. 2014):



$$\frac{\partial}{\partial t} \begin{pmatrix} \rho \\ \rho v \\ E \\ B \end{pmatrix} + \nabla \cdot \begin{pmatrix} \rho v \\ \rho v v - \frac{B B}{\mu} \\ (E + pt)v - \frac{B}{\mu}(v \cdot B) \\ v B - B v \end{pmatrix} = \begin{pmatrix} 0 \\ \rho g \\ \rho v \cdot g \\ 0 \end{pmatrix}$$

In the above representation of the set of ideal MHD equations, the symbol ρ depicts mass density, v denotes the velocity, B is the magnetic-field satisfying the $\nabla \cdot B = 0$ divergence free condition, μ depicts the magnetic permeability. The parameter $pt = p + B^2/(2\mu)$ defines the total pressure which is an addition of the thermal(p) and magnetic ($B^2/2$) pressure. \mathbf{I} is the 3×3 unit matrix. The quantity E describes the total energy which is given as follows (Mignone et al., 2007, 2012; Wołoszkiewicz et al. 2014):

$$E = \frac{p}{\gamma-1} + \frac{\rho v^2}{2} + \frac{B^2}{2\mu}.$$

In this equation, γ is the specific heats ratio. PLUTO code also satisfies an ideal gas equation under the MHD regime where we do not consider the microscopic interactions of the particles at considered length scale:

$$p = \frac{k_B}{m} \rho T$$

In this equation, T symbolizes temperature while K_B is the Boltzmann constant. The symbol m denotes the mean particle mass. We take typical value of m for the model atmosphere that is equals to 1.24 . We do not consider the non-ideal conditions such as velocity of background plasma flows, dissipative effects like viscosity and resistivity, magnetic diffusivity, cooling and/or heating of the plasma, because we are interested in understanding the kinematics and evolutionary properties of jets. We consider the $\nabla \cdot B$ equals to Zero or a very negligible values in the numerical domain.

2.1 Equilibrium Model of the Solar Atmosphere

We consider the numerical simulation box mimicking a realistic solar atmosphere covering the region from the photosphere to the inner corona. In the case of the solar atmosphere subjected to the hydrostatic equilibrium, the realistic temperature profile $T(y)$ is shown in Fig. 2, which is attributed by the measurement of Avrett and Loeser (2008), and also depicted in Konkol et al. (2012).

In the case of the static equilibrium of the solar atmosphere, i.e., when there is no background flows initially ($V_e = 0$), it is approximated as force free as well as current free magnetic field. Therefore, we can abbreviate the initial magnetic field conditions as

$$\nabla \times B_e = 0, \text{ and } (\nabla \times B_e) \times B_e = 0.$$

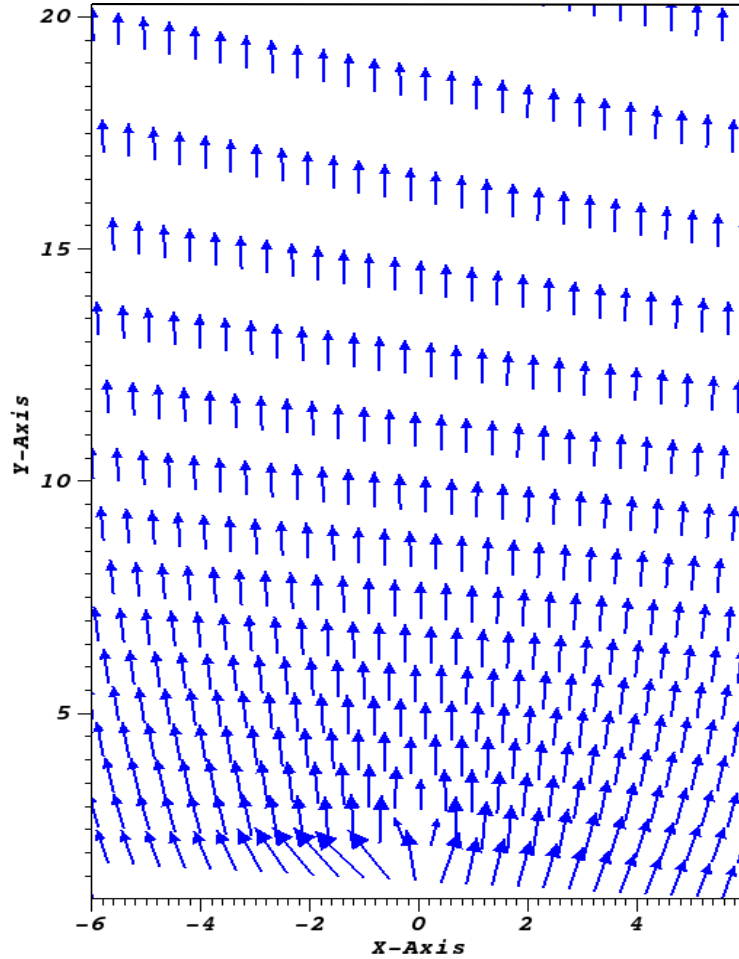


Figure 1. Equilibrium magnetic field lines in the model solar atmosphere. X-axis and Y-axis are given in Mm.

In the given expression, the subscript 'e' represents the equilibrium quantities. The vector magnetic potential can be estimated with the magnetic flux function given as (Konkol et al. 2012):

$$B_e(x, y) = [B_{ex}, B_{ey}, 0] = \nabla \times (A_e \hat{z})$$

5 and

$$A_e(x, y) = \frac{x(y_{ref} - b)^2}{(x-a)^2 + (y-b)^2}$$

In the above mentioned expression, we fix the vertical coordinate of magnetic pole, $b = -5$ Mm in the convection zone. The reference level is taken in the overlying corona at $y_{ref} = 10$ Mm. The magnetic field lines exhibit open and expanding field



behaviour as shown in Fig. 1. We take the magnetic field strength typical of the regions at the Sun where chromospheric jets are formed in the quiet-Sun.

In the hydrostatic equilibrium of the solar atmosphere set in the simulation box, the gravity force balances the pressure gradient force. This can be written as follows:

5

$$-\nabla p + \rho g = 0$$

Here we keep fix the value g as $27400.0 \text{ cm s}^{-2}$. Using the vertical component of the hydrostatic equilibrium in the model solar atmosphere and ideal law, we determine the equilibrium plasma gas pressure and mass density as follows:

10

$$p(y) = p_{ref} \exp\left(-\int_{y_{ref}}^y \frac{dy'}{\Lambda(y')}\right), \rho(y) = \frac{p(y)}{g\Lambda(y)},$$

where

$$\Lambda(y) = \frac{k_B T(y)}{m g},$$

In these expressions, P_{ref} is the gas pressure at reference level y_{ref} , which is attributed as the pressure scale height.

For considering the gravitationally stratified and longitudinally structured solar atmosphere, We obtain the plasma temperature profile $T(y)$ which is derived by Avrett and Loeser (2008) and displayed in Fig.2. It should be noted that the typical value of the temperature $T(y)$ at the top of the photosphere is about 5700 K. This temperature corresponds to $y = 0.5 \text{ Mm}$ at the photosphere, while it falls gradually and attain its minimum about 4350 K at higher altitudes about $y = 0.95 \text{ Mm}$ which represents temperature minimum. As we move higher up in the solar atmosphere, $T(y)$ increases gradually with the height up to the transition region which is located at $y \simeq 2.7 \text{ Mm}$. $T(y)$ sharply increases up to the corona and finally attains the constant value of mega-Kelvin at the coronal heights as shown in Fig. 2.

15
20

2.1.1 Perturbations

We consider the initial solar atmosphere as in the hydrostatic equilibrium and gravitationally-stratified. We perturb the equilibrium atmosphere by the initial pulse in the vertical direction in equilibrium pressure. The Gaussian form of the pressure pulse in the vertical direction is given as follows:

25

$$P = P_0 \left(1 + A_p \times \exp\left(-\frac{(x-x_0)^2 + (y-y_0)^2}{\omega^2}\right)\right),$$

Here (x_0, y_0) is initial position of the pressure pulse. ω is the width of the pulse, and A_p denotes the pressure amplitude. We fix the value of x_0, y_0 as 0 and 1.8 Mm respectively, therefore, launching the pressure perturbations in the chromosphere. We take ω equals to 0.2 Mm. We imply different pressure pulse strength $A_p = 4-22$, which account for the generation of the variety of solar jets.

30

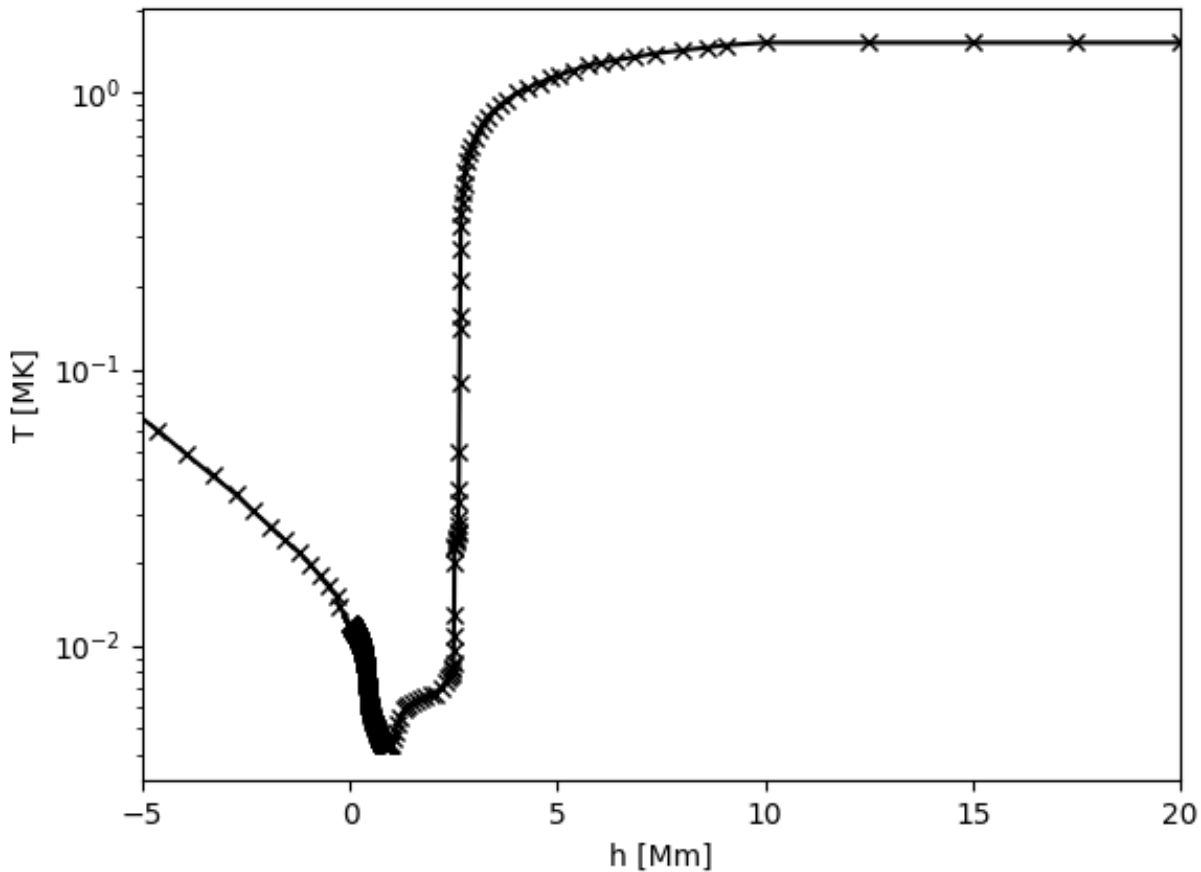


Figure 2. Temperature variation with the height in the initial static solar atmosphere.

2.2 Numerical Methods

PLUTO code is a Godunov-type, non-linear, finite-volume and finite-difference magnetohydrodynamic (MHD) code which takes into account ideal and non-ideal sets of governing equations (cf., Mignone et al., 2007, 2012, Wołoszkiewicz et al. 2014). It is constructed to integrate numerically a system of conservation laws, which can be shown as follows:

5

$$\frac{\partial U}{\partial t} + \nabla \cdot F(U) = S(U) \quad \dots (1)$$

In this equation, U denotes a set of conservative physical fields (e.g., magnetic field, density, velocity, pressure etc), while $F(U)$ is the flux tensor and $S(U)$ is the source term.



PLUTO code considers to utilize a second-order unsplit Godunov solver and Adaptive Mesh Refinement (AMR) of the system of conservation laws as shown in the Eq.(1). In order to solve the set of ideal MHD equations (Eq.1) numerically, we set the simulation box as $(-6, 6) \text{ Mm} \times (1, 21) \text{ Mm}$. This represents a realistic localized solar atmosphere of 12 Mm and 20 Mm span respectively in the horizontal and vertical directions. This solar atmosphere is constructed within the simulation box, and all four boundary conditions by fixing the simulation region to their equilibrium values. Numerical simulation is done with double precision arithmetic using multiple passage interface (MPI) (see Mignone et al., 2007). The eight processors are used in the parallel calculations. It took approximately 12 hours of CPU time for each set of the calculations. We adopted a static uniform grid which is divided into 384 equal cells in x-direction. We also adopted a static uniform and stretched grid which are divided into 128 equal and 256 equal cells respectively in y-direction. The resolution of the simulation domain is 31 km per numerical cell. We have obtained the numerical simulation data every 10 seconds.

In our modelling, we set the Courant-Friedrichs-Lewy number equals to 0.25. We use Roe solver for the flux computation, which is linearized Riemann solver based on the characteristic decomposition of the Roe matrix (cf., Mignone et al., 2007, 2012, Woloszkiwicz et al. 2014).

3 Results

The pressure perturbations in the solar chromosphere launches the thin and localized plasma jets (Fig. 3). These jets carry the mass from the chromosphere to the outer corona along the expanding open field lines. The pressure perturbations mimic the impulsive origin of these jets due to the localized heating episodes that might occur at some time epoch in the solar chromosphere and that cause the direct pressure disturbance in the equilibrium atmosphere. As the pressure pulse is launched, the plasma gets essential velocity perturbations guided along the vertical and expanding field lines. These perturbations are converted in magneto acoustic shocks in the stratified atmosphere which is followed by the motion of plasma behind forming the jet. Shock leaves the domain quickly, and resulting effect that remains behind is the formation of the jet.

We have analyzed the kinematical and evolutionary properties of these pressure pulse driven solar jets. Fig. 5 displays the height-time profile of various jets. It shows that the jets exhibit asymmetric parabolic paths, which is different than the normal parabolic path of any ejecta in the gravitational field. We develop a code in Matlab to find the height of the jet with time. For calculating the height of the jet we took the time-series of the numerical simulation data (Fig.4a). In the density map, we estimate the assigned RGB values showing the density variations over the colour scales. Highest density corresponds to the fixed value of green with $G=255$ and the value of it decreases towards blue (B) as we go towards the tip of the jet with decreasing density. Ultimately it becomes 245 as the jet ends although it fades away slowly and there is no sharp boundary, so we took $B=245$ as the approximate boundary value for the jet. So we have used this observation to calculate the required parameters by fixing $G=255$, $B \leq 245$ and generated a masked image with only $G=255$, $B \leq 245$ and rest of the portion as black (Fig.4b). Then we have generated the contour of the masked image to get (Fig.4c) and then we found the height variations automatically w.r.t. time. We took the snapshots of density map for the calculation of height when the jet has rise above the transition region and the snapshots of pressure map for the calculation of the height of the jet when it is below the transition

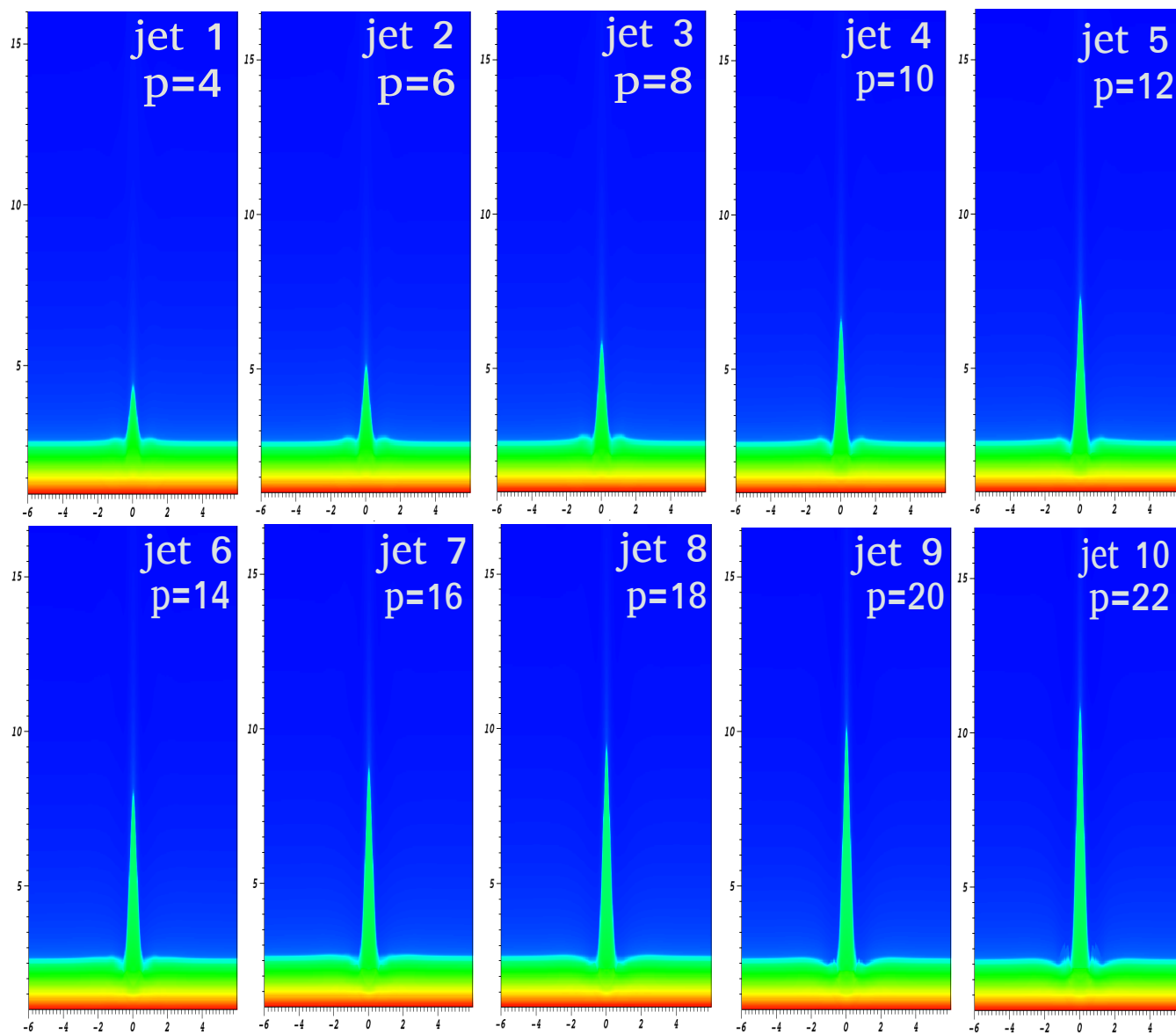


Figure 3. Evolution of the plasma jets at different pressure pulse. The Mosaic diagram shows the maximum height of the evolved jets at different pressure pulses, e.g., $p=4$, $p=6$, $p=8$, $p=10$, $p=12$, $p=14$, $p=16$, $p=18$, $p=20$ and $p=22$. Horizontal (x) and vertical (y) axes are in Mm.

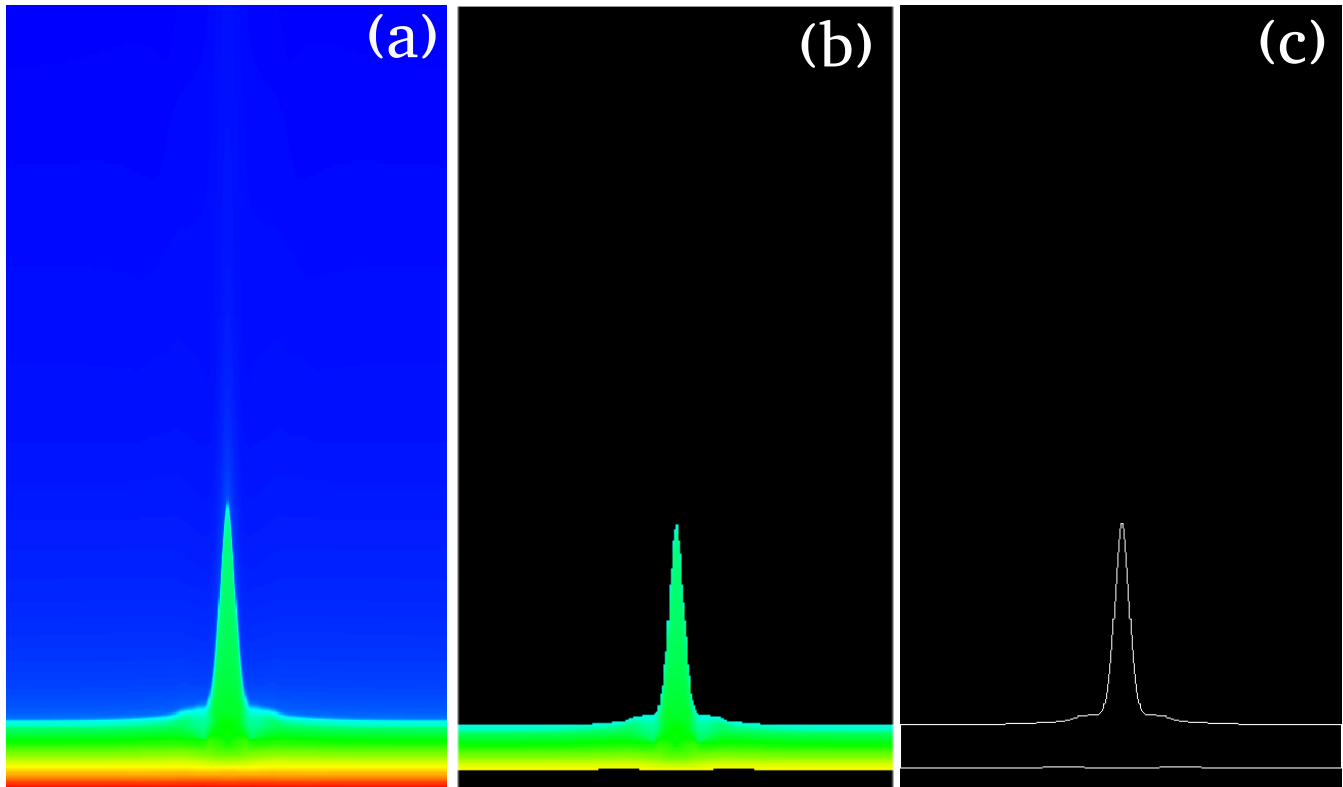


Figure 4. Automated detection of the plasma jet in the numerical simulation data to establish its time-distance profile and termination point.

region. Also at the time $t=0$ s, we took the value of height as 1.8 Mm as was set for simulation. The lifetime of the isolated jet is estimated in the masked time-series where only the jet's motion is visible. We calculate the time when the height of the jet again starts increasing after the fall, and this point we consider the termination point of the first isolated jet. For $P=14$ (time=190 sec Density Map), we have demonstrated the above mentioned procedure in Fig. 4.

- 5 The automatically detected height-time profiles for the jets originated by imposing different pressure pulses clearly exhibit the asymmetric near parabolic profile (Fig. 5). This infers that the upward motion of the jet under the influence of pressure perturbations does occur, however, its downward motion is not singly governed by the gravitational free fall. The downward propagating counterpart of the perturbation when reflects from the photosphere, it goes up and causes its interaction with the falling jet plasma. This creates the complex scenario near the base of the jet where we observe the complex plasma motion and
- 10 evolution of the multiple jets one by one (e.g., Murawski et al. 2011; Kayshap et al. 2018, Li et al. 2019). Fig. 6 displays an interesting correlation between maximum height of the jets and strength of the pressure pulse, which shows a linear increasing trend. This directly infers that if the extent of the heating and thus pressure perturbations will be higher then the more longer jets can be generated from the same location in the chromosphere. The width of the jets is determined by the conservation of mass in the cross section of the flowing jet spire, however, many other factors, i.e., the configuration of the magnetic field,

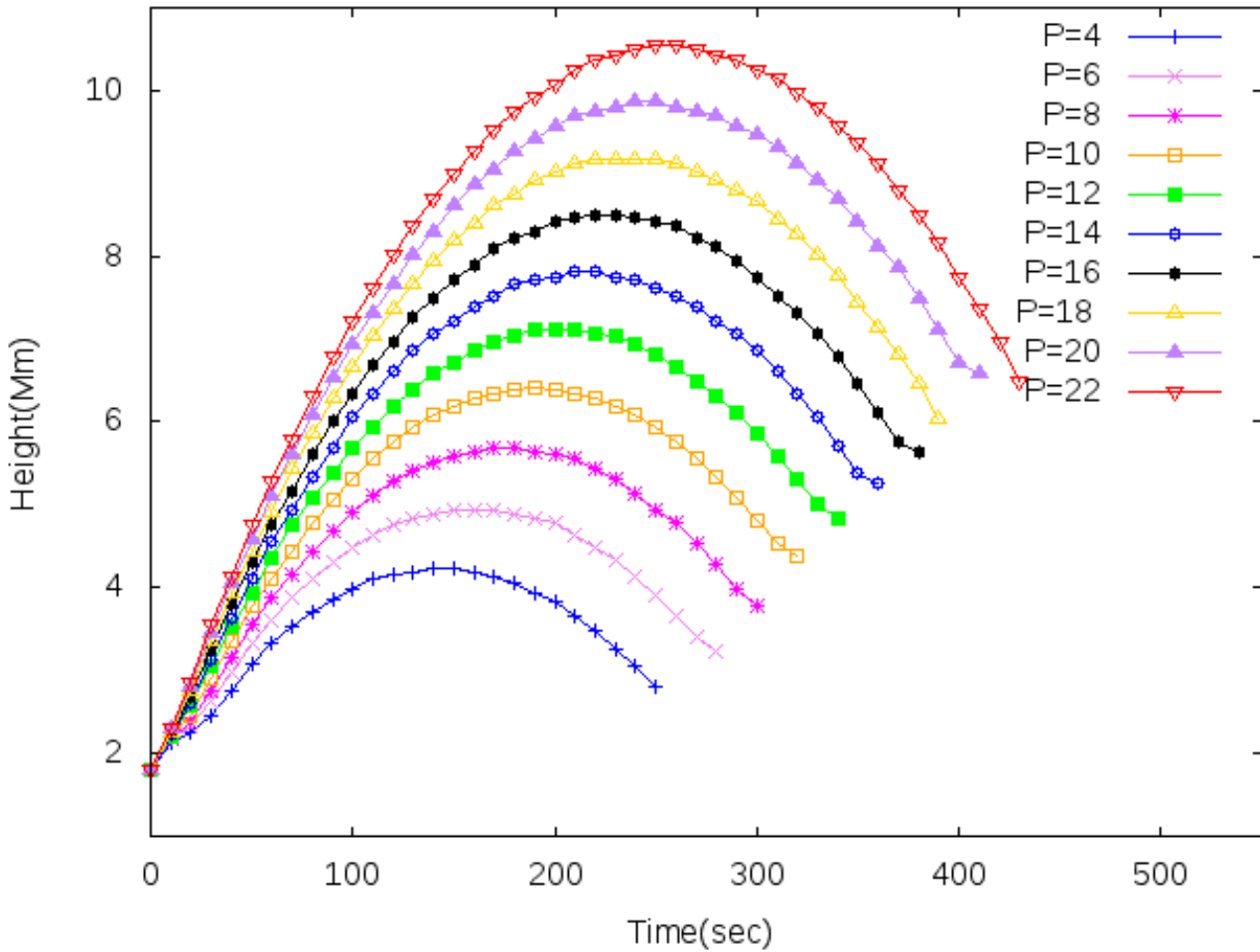


Figure 5. Height of the jets and their evolution w.r.t. the time.

the interaction of counter-propagating disturbances near the base of the jet etc can affect it. We find in general linear fitted trend with negative slope on the variation of the jet's width w.r.t pressure pulse strength (Fig. 7). The life-time of the jets shows linear variation with a positive slope w.r.t. the pressure pulse strength. These scenarios clarify that the more the localized energy release in the chromosphere, the more larger perturbation will lead longer and well collimated jets which will also have greater

5 life time.

4 Conclusions

There are several jets in the chromosphere (e.g., macrospicules, network jets, isolated repeated jets, confined surges; Wilhelm 2000; Murawski et al. 2011; Uddin et al. 2012; Kayshap et al. 2013b,2018, Li et al. 2019, and referencec cited therein). The

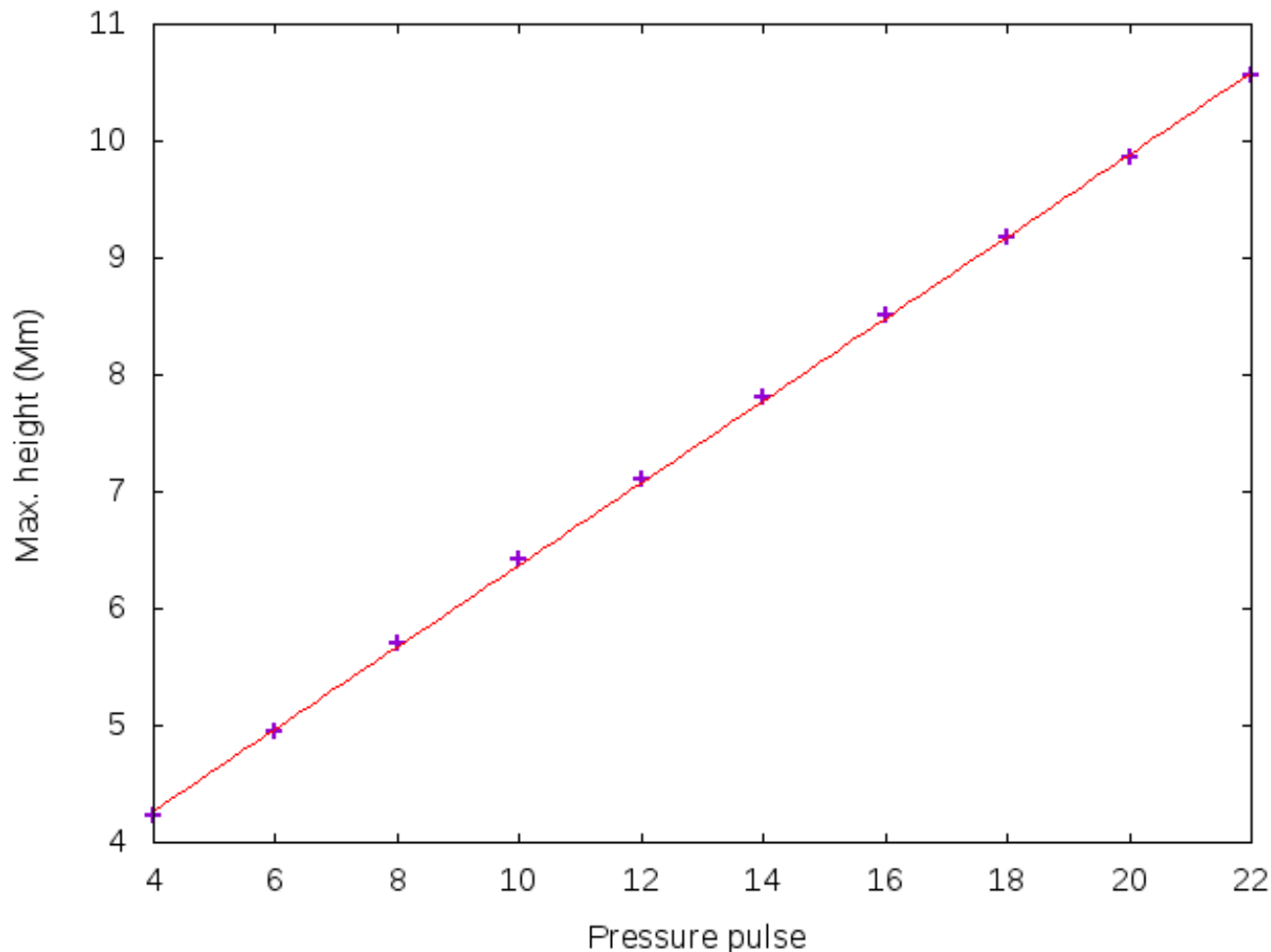


Figure 6. Maximum height of the model jets vs. pressure pulse strength.

common resemblance point in the evolution of these jets is the presence of heating at their base. Sometimes these jets are so abundant that they over-impose on the co-spatial presence of classical chromospheric ejecta like type-I and type-II spicules (Tian et al. 2014). Therefore, we can not ignore the role of such episodic jets in determining the mass as well as energy transport in the corona. It should be noted that we attempt here to model the above mentioned episodic and impulsive jets in terms of their kinematical and evolutionary properties. However we exclude the classical chromospheric spicules (type-I and type-II), spicule-like structures, anemone jets, etc in this physical model as they may require additional driving mechanisms for their launch and in the non-linear regime complex plasma flows, and wave activity may present there (e.g., De Pontieu et al. 2004; Shetye et al. 2016; Srivastava et al. 2017; Martínez-Sykora et al. 2017, and references cited there). Therefore, we simply

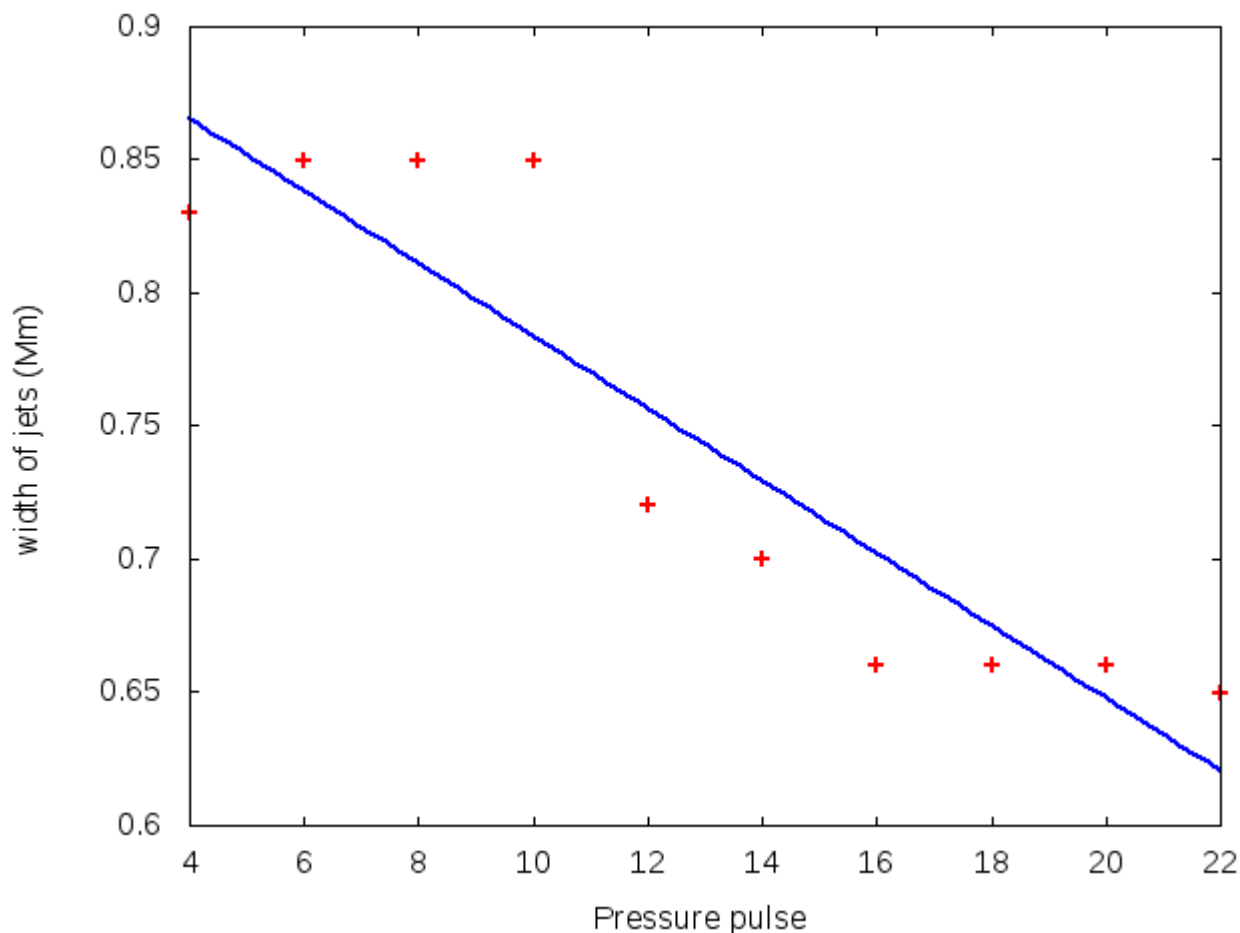


Figure 7. Width of the jets at their maximum heights vs. pressure pulse strength.

include those jets and their kinematical properties in our model, which evolve due to heating at their footpoints and associated pressure pulse.

It should be noted that our results demonstrate that the elongation and life-time of these jets are directly proportional to the heating pulse, and their shape depends upon the complex plasma motions near their base as well as magnetic field configurations of their spire. Therefore, in general we see the brightening and mass motions starting at their base and evolution of the plasma motion occurs at the Jet's spire. Our model represents the formation of such chromospheric jets which are evolved due to the pressure perturbations near their footpoints. Although, we present the kinematics and evolutionary properties of the a single isolated jet, but usually such sites where pressure perturbations do occur, exhibits the formation of the multiple jets along with the significant brightening at their base. Such locations are very common sites for the origin of the impulsively triggered isolated chromospheric jets as mentioned above.

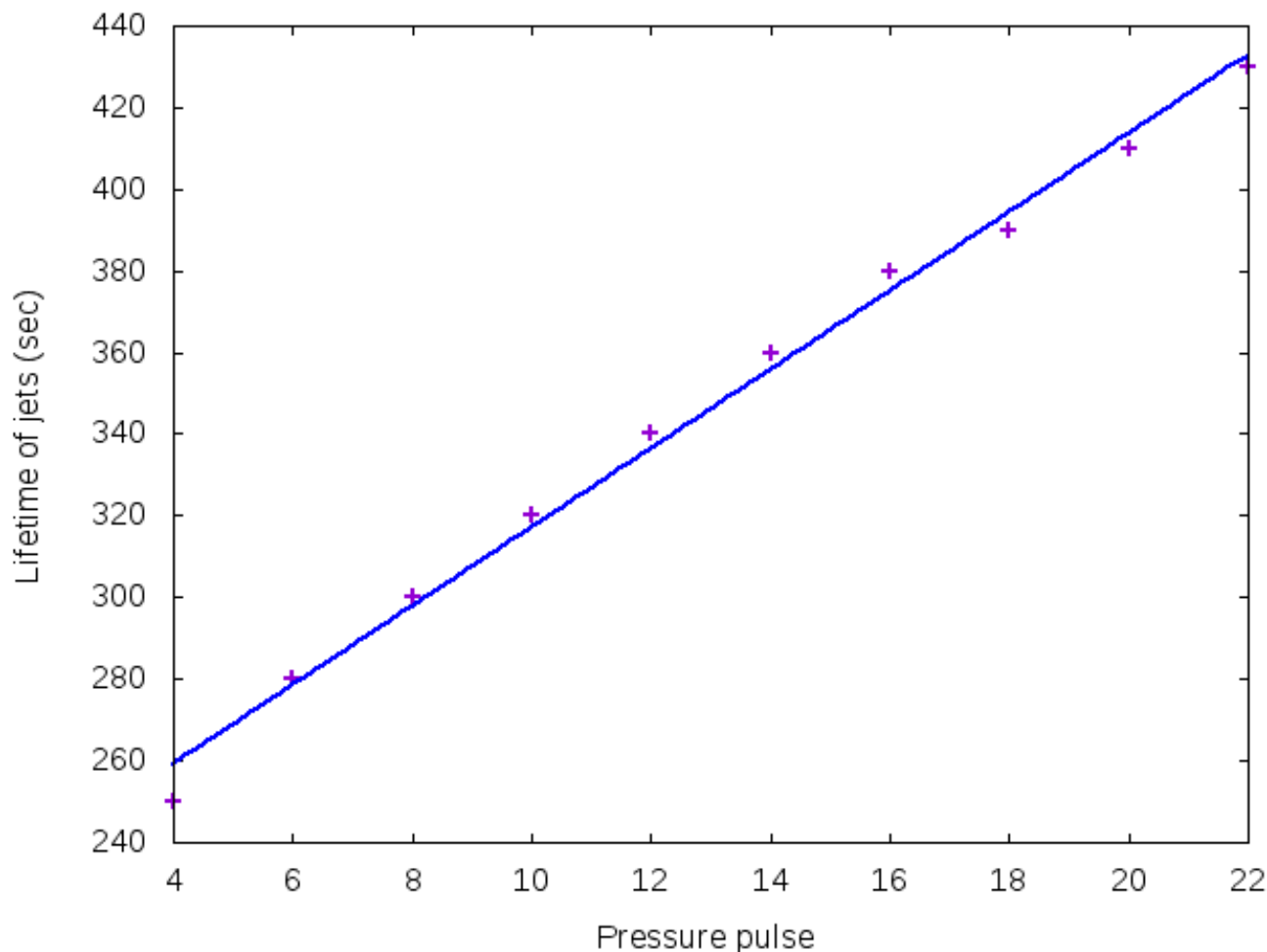


Figure 8. Life-time of the model jets vs. pressure pulse strength.

Author contributions. All authors have contributed in a equal manner.

Competing interests. There is no competing interest in the authors.

Acknowledgements. We acknowledge the UKIERI Research grant provided by University Grant Commission (UGC), India and British Council, UK for the support of current research. We thankfully acknowledge the support of Dr. P. Konkol and Prof. K. Murawski, UMCS, Lublin, Poland for providing their support on providing realistic solar atmosphere to incorporate with the PLUTO code. Finally, we acknowledge the use of PLUTO code in our present work.



References

- De Pontieu, B., Erdélyi, R., & James, S. P.: Solar chromospheric spicules from the leakage of photospheric oscillations and flows, *Nature*, 430, 536, 10.1038/nature02749, 2004
- De Pontieu, B., McIntosh, S. W., Carlsson, M., Hansteen, V. H., Tarbell, T. D., Schrijver, C. J., Title, A. M., Shine, R. A., Tsuneta, S., Katsukawa, Y., Ichimoto, K., Suematsu, Y., Shimizu, T., Nagata, S.: Chromospheric Alfvénic Waves Strong Enough to Power the Solar Wind, *Science*, 318, 1574, 10.1126/science.1151747, 2007
- Iijima, H., & Yokoyama, T.: A Three-dimensional Magnetohydrodynamic Simulation of the Formation of Solar Chromospheric Jets with Twisted Magnetic Field Lines, *Astrophys. J.*, 848, 38, 10.3847/1538-4357/aa8ad1, 2017
- Jelínek, P., Srivastava, A. K., Murawski, K., Kayshap, P., & Dwivedi, B. N.: Spectroscopic observations and modelling of impulsive Alfvén waves along a polar coronal jet, *Astron. Astrophys.*, 581, A131, 10.1051/0004-6361/201424234, 2015
- Katsukawa, Y., Berger, T. E., Ichimoto, K., Lites, B. W., Nagata, S., Shimizu, T., Shine, R. A., Suematsu, Y., Tarbell, T. D., Title, A. M., Tsuneta, S.: Small-Scale Jetlike Features in Penumbral Chromospheres, *Science*, 318, 1594, 10.1126/science.1146046, 2007
- Kayshap, P., Murawski, K., Srivastava, A. K., & Dwivedi, B. N.: Rotating network jets in the quiet Sun as observed by IRIS, *Astron. Astrophys.*, 616, A99, 10.1051/0004-6361/201730990, 2018
- Kayshap, P., Srivastava, A. K., & Murawski, K.: The Kinematics and Plasma Properties of a Solar Surge Triggered by Chromospheric Activity in AR11271, *Astrophys. J.*, 763, 24, 10.1088/0004-637X/763/1/24, 2013a
- Kayshap, P., Srivastava, A. K., Murawski, K., & Tripathi, D.: Origin of Macrospicule and Jet in Polar Corona by a Small-scale Kinked Flux Tube, *Astrophys J. Lett.*, 770, L3, 10.1088/2041-8205/770/1/L3, 2013b
- Konkol, P., Murawski, K., & Zaqarashvili, T. V.: Numerical simulations of magnetoacoustic oscillations in a gravitationally stratified solar corona, *A&A*, 537, A96, 10.1051/0004-6361/201117943, 2012
- Li, X., Zhang, J., Yang, S., & Hou, Y.: Flow Instabilities in Solar Jets in Their Upstream and Downstream Regimes, *ApJ*, 875, 52, 10.3847/1538-4357/ab0f39, 2019
- Martínez-Sykora, J., De Pontieu, B., Hansteen, V. H., Rouppe van der Voort, L., Carlsson, M., Pereira, T. M. D.: On the generation of solar spicules and Alfvénic waves, *Science*, 356, 1269, 10.1126/science.aah5412, 2017
- McIntosh, Scott W., de Pontieu, Bart, Carlsson, Mats, Hansteen, Viggo, Boerner, Paul, Goossens, Marcel.: Alfvénic waves with sufficient energy to power the quiet solar corona and fast solar wind, *Nature*, 475, 477, 10.1038/nature10235, 2011
- Mignone, A., Bodo, G., Massaglia, S., Matsakos, T., Tesileanu, O., Zanni, C., Ferrari, A.: PLUTO: A Numerical Code for Computational Astrophysics, *ApJS*, 170, 228, 10.1086/513316, 2007
- Mignone, A., Zanni, C., Tzeferacos, P., van Straalen, B., Colella, P., Bodo, G.: The PLUTO Code for Adaptive Mesh Computations in Astrophysical Fluid Dynamics, *ApJS*, 198, 7, 10.1088/0067-0049/198/1/7, 2012
- Murawski, K., Kayshap, P., Srivastava, A. K., Pascoe, D. J., Jelínek, P., Kuźma, B., Fedun, V.: Magnetic swirls and associated fast magnetoacoustic kink waves in a solar chromospheric flux tube, *Mon. Not. Royal Astron. Soc.*, 474, 77, 10.1093/mnras/stx2763, 2018
- Murawski, K., Srivastava, A. K., & Zaqarashvili, T. V.: Observations of Chromospheric Anemone Jets with Hinode Ca II Broadband Filtergraph and Hida Ca II Spectroheliograph, *A&A*, 535, A58, 10.1093/pasj/62.4.901, 2011
- Morita, Satoshi, Shibata, Kazunari, UeNo, Satoru, Ichimoto, Kiyoshi, Kitai, Reizaburo, Otsuji, Ken-ichi.: Observations of Chromospheric Anemone Jets with Hinode Ca II Broadband Filtergraph and Hida Ca II Spectroheliograph, *Pac. Astron. Soc. Japan*, 62, 901, 10.1093/pasj/62.4.901, 2010



- Nishizuka, N., Shimizu, M., Nakamura, T., Otsuji, K., Okamoto, T. J., Katsukawa, Y., Shibata, K.: Giant Chromospheric Anemone Jet Observed with Hinode and Comparison with Magnetohydrodynamic Simulations: Evidence of Propagating Alfvén Waves and Magnetic Reconnection, *Astrophys. J. Lett.*, 683, L83, 10.1086/591445, 2008
- Nisticò, G., Bothmer, V., Patsourakos, S., & Zimbardo, G.: Characteristics of EUV Coronal Jets Observed with STEREO/SECCHI, *Sol. Phys.*, 259, 87, 10.1007/s11207-009-9424-8, 2009
- 5 Raouafi, N. E., Patsourakos, S., Pariat, E., Young, P. R., Sterling, A. C., Savcheva, A., Shimojo, M., Moreno-Insertis, F., DeVore, C. R., Archontis, V., Török, T., Mason, H., Curdt, W., Meyer, K., Dalmasse, K., Matsui, Y.: Solar Coronal Jets: Observations, Theory, and Modeling, *Space Sci. Rev.*, 201, 1, 10.1007/s11214-016-0260-5, 2016
- Roy, J. R.: The Magnetic Properties of Solar Surges, *Sol. Phys.*, 28, 95, 10.1007/BF00152915, 1973
- 10 Shetye, J., Doyle, J. G., Scullion, E., Nelson, C. J., Kuridze, D., Henriques, V., Woeger, F.; Ray, T.: High-cadence observations of spicular-type events on the Sun, *Astron. Astrophys.*, 589, A3, 10.1051/0004-6361/201527505, 2016
- Shibata, Kazunari, Nakamura, Tahei, Matsumoto, Takuma, Otsuji, Kenichi, Okamoto, Takenori J., Nishizuka, Naoto, Kawate, Tomoko, Watanabe, Hiroko, Nagata, Shin'ichi, UeNo, Satoru, Kitai, Reizaburo, Nozawa, Satoshi, Tsuneta, Saku, Suematsu, Yoshinori, Ichimoto, Kiyoshi, Shimizu, Toshifumi, Katsukawa, Yukio, Tarbell, Theodore D., Berger, Thomas E., Lites, Bruce W. Shine, Richard A., Title, Alan
- 15 M.: Chromospheric Anemone Jets as Evidence of Ubiquitous Reconnection, *Science*, 318, 1591, 10.1126/science.1146708, 2007
- Shibata, K., Nishikawa, T., Kitai, R., & Suematsu, Y.: Numerical Hydrodynamics of the Jet Phenomena in the Solar Atmosphere - Part Two - Surges, *Sol. Phys.*, 77, 121, 10.1007/BF00156100, 1982
- Srivastava, Abhishek Kumar, Shetye, Juie, Murawski, Krzysztof, Doyle, John Gerard, Stangalini, Marco, Scullion, Eamon, Ray, Tom, Wójcik, Dariusz Patryk, Dwivedi, Bhola N.: High-frequency torsional Alfvén waves as an energy source for coronal heating, *Scientific Reports*, 20 7, 43147, 10.1038/srep43147, 2017
- Srivastava, Abhishek Kumar, Murawski, Krzysztof, Kuźma, Blażej, Wójcik, Dariusz Patryk, Zaqarashvili, Teimuraz V., Stangalini, Marco, Musielak, Zdzislaw E., Doyle, John Gerard, Kayshap, Pradeep, Dwivedi, Bhola N.: Confined pseudo-shocks as an energy source for the active solar corona, *Nature Astronomy*, 2, 951, 10.1038/s41550-018-0590-1, 2018
- Sterling, A. C.: Solar Spicules: A Review of Recent Models and Targets for Future Observations - (Invited Review), *Sol. Phys.*, 196, 79, 25 10.1023/A:1005213923962, 2000
- Tian, H., DeLuca, E. E., Cranmer, S. R., De Pontieu, B., Peter, H., Martínez-Sykora, J., Golub, L., McKillop, S., Reeves, K. K., Miralles, M. P., McCauley, P., Saar, S., Testa, P., Weber, M., Murphy, N., Lemen, J., Title, A., Boerner, P., Hurlburt, N., Tarbell, T. D. Wuelser, J. P., Kleint, L., Kankelborg, C., Jaeggli, S., Carlsson, M., Hansteen, V., McIntosh, S. W.: Prevalence of small-scale jets from the networks of the solar transition region and chromosphere, *Science*, 346, 1255711, 10.1126/science.1255711, 2014
- 30 Uddin, Wahab, Schmieder, B., Chandra, R., Srivastava, Abhishek K., Kumar, Pankaj, Bisht, S.: Observations of Multiple Surges Associated with Magnetic Activities in AR 10484 on 2003 October 25, *Astrophys. J.*, 752, 70, 10.1088/0004-637X/752/1/70, 2012
- Wedemeyer-Böhm, Sven, Scullion, Eamon; Steiner, Oskar, Rouppe van der Voort, Luc, de La Cruz Rodriguez, Jaime, Fedun, Viktor, Erdélyi, Robert.: Magnetic tornadoes as energy channels into the solar corona, *Nature*, 486, 505, 10.1038/nature11202, 2012
- Wilhelm, K.: Solar spicules and macrospicules observed by SUMER, *Astron. Astrophys.*, 360, 351, 2000
- 35 Woloszkiwicz, P., Murawski, K., Musielak, Z.E., and Mignone, A.: Numerical simulations of Alfvén waves in the solar atmosphere with the PLUTO code, *Control & Cybernetics*, 43, 2, 2014
- Yokoyama, T., & Shibata, K.: Magnetic reconnection as the origin of X-ray jets and H α surges on the Sun, *Nature*, 375, 42, 10.1038/375042a0, 1995